Pathogen Detection

DOI: 10.1002/anie.201307952

Acetylcholinesterase-Catalyzed Hydrolysis Allows Ultrasensitive Detection of Pathogens with the Naked Eye**

*Dingbin Liu, Zhantong Wang, Albert Jin, Xinglu Huang, Xiaolian Sun, Fu Wang, Qiang Yan, Shengxiang Ge, Ningshao Xia, Gang Niu, Gang Liu, A. R. Hight Walker, and Xiaoyuan Chen**

We present a colorimetric assay for pathogen detection based on a acetylcholinesterase (AChE)-catalyzed hydrolysis reaction with ultrahigh sensitivity that is comparable to the sensitivity of polymerase chain reaction (PCR). The rapid detection of pathogens is essential for timely clinical decision-making and management of epidemics of infectious diseases. In resource-constrained settings, however, it still remains a great challenge to identify and control the outbreak of infectious diseases at their earliest stages because of the lack of convenient and reliable diagnostic technologies.[1]

Over the past decades, many approaches have been developed for pathogen detection, including loop-mediated isothermal amplification (LAMP),[2] electrochemistry,[3] and nanotechnology,[4] just to name a few. However, most detection systems fail to monitor the pathogens in clinical samples, where their concentrations are generally very low. Presently, PCR amplification of viral RNA has been used as the gold standard for molecular identification of infectious diseases.[5] Although the PCR strategy exhibits ultrahigh sensitivity for pathogen detection, it requires expensive instruments and reagents, and skilled labor, which limits its applications in remote settings, such as developing countries where acute infections appear to be increasing in recent years. Therefore, it is urgent to develop a high-sensitivity approach that can act as an alternative to PCR for pathogen detection.

Herein, we describe an ultrasensitive colorimetric assay aimed at providing rapid detection of pathogens, and demonstrate its utility in clinical samples. This sensing platform is based on an improved heterogeneous sandwich-type enzyme-linked immunosorbent assay (ELISA). In this study, the detection sensitivity is expected to be considerably enhanced due to two rounds of amplification. In the first round, detection antibodies (denoted as Ab2) were conjugated with AChE, which catalyzes its substrate acetylthiocholine (ATC, an analogue of acetylcholine) to generate thiocholine. Thiocholine can induce aggregation of citrate-capped gold nanoparticles (citrate-AuNPs) through electrostatic interactions. This aggregation event can be reflected by the color change of the AuNP solutions from red to purple, which can be observed by the naked eye (Figure 1).[6] In the second round, magnetic beads (MBs) were used to load many thousands of AChE (31000 AChE per MB in this study) and Ab2. This Ab2-AChE-MB format can specifically

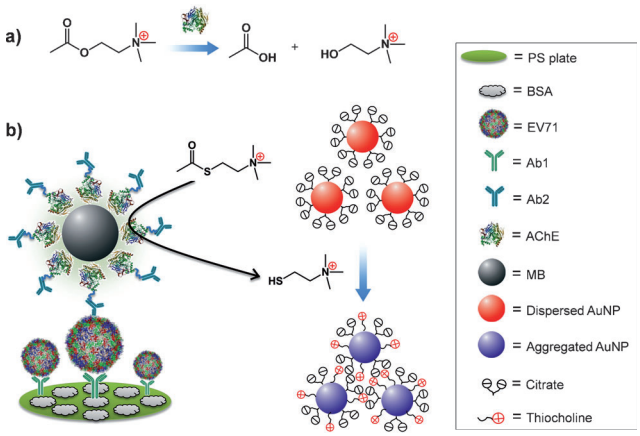

Figure 1. The AChE-catalyzed hydrolysis reaction for the colorimetric detection of enterovirus 71 (EV71). a) AChE catalyzes the hydrolysis of acetylcholine to generate acetate and choline. b) The improved sandwich ELISA format. EV71 is pulled down onto the polystyrene (PS) substrate by a capture antibody (Ab1) and recognized by a detection antibody (Ab2) that which was conjugated with AChE onto the magnetic beads (MB). In the presence of acetylthiocholine (ATC) and citrate-covered AuNPs, AChE catalyzes the hydrolysis of ATC to generate thiocholine, thus inducing the aggregation of AuNPs through electrostatic interaction.

[*] D. Liu, X. Huang, X. Sun, F. Wang, G. Niu, Dr. X. Chen
Laboratory of Molecular Imaging and Nanomedicine (LOMIN)
National Institute of Biomedical Imaging and Bioengineering (NIBIB), National Institutes of Health (NIH)
Bethesda, MD 20892 (USA)
E-mail: shawn.chen@nih.gov

Z. Wang, Q. Yan, S. Ge, Prof. N. Xia
National Institute of Diagnostics and Vaccine Development in Infectious Disease, School of Public Health, Xiamen University
Xiamen 361102 (China)

Z. Wang, G. Liu
Center for Molecular Imaging and Translational Medicine, School of Public Health, Xiamen University, Xiamen 361005 (China)

Dr. A. Jin
Laboratory of Cellular Imaging and Macromolecular Biophysics
National Institute of Biomedical Imaging and Bioengineering
National Institutes of Health, Bethesda, MD 20982 (USA)

Dr. A. R. Hight Walker
Optical Technology Division, Physics Laboratory, National Institute of Standards and Technology, Gaithersburg, MD 20899 (USA)

[**] This work was supported in part the Major State Basic Research Development Program of China (973 Program; 2013CB733802 and 2014CB744503), the National Science Foundation of China (NSFC; 81101101, 51273165, 81201086, 81201190, and 81371596), a Key Project of the Chinese Ministry of Education (212149), the Intramural Research Program (IRP) of the National Institute of Biomedical Imaging and Bioengineering (NIBIB), and the National Institutes of Health (NIH). D.L. was supported by a postdoctoral fellowship from NIH-NIBIB/NIST NRC.

Supporting information for this article is available on the WWW under http://dx.doi.org/10.1002/anie.201307952.

recognize the analyte that was captured by the capture antibody (denoted as Ab1). Very small amounts of the analytes can thus be detected because of the high density of AChE on MB where the AChE activity is highly maintained.

We first demonstrated that thiocholine is capable of inducing the aggregation of citrate-AuNPs. By incubating citrate-AuNPs (15 nm in diameter, 2.3 nM) with 1 μM of thiocholine (2-mercapto-*N*,*N*,*N*-trimethylethanaminium; 2-MTA), the chemisorbed citrate molecules can be partially removed from the Au surface by means of ligand exchange, and finally the thiol ligands can be adsorbed onto the Au surfaces through Au–S bonds.[7] The positively charged groups of the ligands may interact with the negatively charged citrate residues that still cover the Au surfaces, thus causing the cross-linking of AuNPs. This process resulted in a color change of the AuNP solution from red to blue and a simultaneous change of the absorption band in the visible region of the electromagnetic spectrum (Supporting Information, Figure S1).

Then, we prepared the Ab2 and AChE-functionalized MB (Ab2-AChE-MB) using a step-by-step procedure (Scheme 1). Firstly, we chose *N*-hydroxysuccinimide (NHS)-activated MB

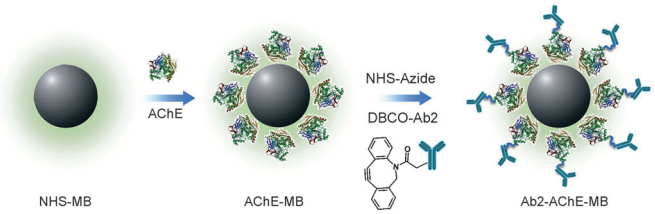

Scheme 1. Procedure for preparation of Ab2-AChE-MB. AChE molecules were coated onto MB through NHS chemistry. The AChE-MB conjugate further reacted with NHS-azide, and was then conjugated with DBCO-Ab2 by copper-free click chemistry to form Ab2-AChE-MB.

to load AChE and used an AChE assay kit to measure the AChE activity before and after conjugation with MB (Figure S2). The results indicate that 89.1 % of the original AChE activity was maintained after conjugation, based on which, the number of AChE on each MB was calculated to be around 31 000, which is similar to previous reports.[8] Later, we attempted to functionlize the AChE layer with Ab2 by copper-free click chemistry. Copper-free click chemistry is an effective strategy to join two molecules in a one-step procedure without generating side products. This strategy depends on the reaction of a dibenzocyclooctyl (DBCO) reagent with an azide linker to form a stable triazole in aqueous buffered media, which is a highly efficient conjugation method.[9] In this study, azide was labeled onto the AChE layer by reaction between an NHS-activated azide and the remainning amines on AChE. The resulting MBs were subsequently conjugated with DBCO-labeled Ab2 (DBCO-Ab2) by means of copper-free click chemistry.

We investigated the sensitivity of the AuNP-based colorimetric assay for Ab2-AChE-MB, and compared it with the conventional AChE assay kit. We first applied the AuNP-based colorimetric assay to measure the activity of Ab2-AChE-MB by serial dilution of the MBs, resulting in final concentrations of $1.0–20 \times 10^3$ particles/mL. The aggregation process of AuNPs can be easily visualized by the color change of AuNP solutions from red to purple (Figure S3 a). Simultaneously, the UV/Vis absorption (Figure S3 b) suggests that, as the Ab2-AChE-MB concentration increases, the absorbance at around 520 nm gradually decreases, along with an increase of the absorbance at 600–800 nm, which indicates the formation of AuNP aggregates. The plot of A_{700}/A_{520} (the ratio of absorbance at 700 nm and 520 nm) versus various concentrations of Ab2-AChE-MB reflected the linear concentration-dependent aggregation process (Figure S3 c). Moreover, we found that the aggregation is a time-dependent process. Figure S4 shows the plots of A_{700}/A_{520} values versus the incubation time (0–10 min) for various concentrations of Ab2-AChE-MB. Within the incubation time, the A_{700}/A_{520} values increased, except for the blank sample, the A_{700}/A_{520} values of which showed negligible changes. By both UV/Vis absorption and the naked eye, the lowest detectable concentration of Ab2-AChE-MB is 1.0×10^3 particles/mL.

To analyze the aggregation process at the nanoscale, we applied transmission electron microscopy (TEM) to characterize the states of AuNPs before and after aggregation induced by Ab2-AChE-MB (Figure S5). The aggregation process was also supported by dynamic light scattering data (Figure S6 a). The average hydrodynamic diameter of the well-dispersed citrate-AuNPs was 29.1 ± 2.51 nm, whereas that of the AuNP aggregates increased to 415.2 ± 23.3 nm, which is congruent with TEM analysis. Additionally, the change of surface charges was monitored by zeta potential measurement (Figure S6 b). As reported elsewhere,[10] the citrate-AuNPs are negative in charge (-35.8 ± 1.9 mV in this study). In the presence of thiocholine (produced by the Ab2-AChE-MB-catalyzed hydrolysis of ATC), the surface charge of AuNPs was neutralized to -2.2 ± 0.9 mV, which was attributed to the positively-charged quaternary ammonium group on thiocholine. All of the measurements strongly supported that a small number of Ab2-AChE-MBs can induce massive aggregation of citrate-AuNPs in the presence of ATC, making this system very promising for the ultrasensitive detection of pathogens.

This AuNP-based colorimetric assay was compared with the conventional AChE assay kit for Ab2-AChE-MB detection. The AChE assay kit is based on an improved Ellman method.[11] The absorbance at 412 nm is proportional to AChE activity. As shown in Figure S7, the lowest detectable concentration of Ab2-AChE-MB using the AChE assay kit was 2.5×10^5 particles/mL (250-fold higher than that of our assay). The high sensitivity of our assay was attributed to the very high extinction coefficient ($10^8–10^{10}$ M^{-1} cm^{-1}) of AuNPs, which is at least three orders of magnitude higher than those of common organic dyes.[12]

After demonstrating that the colorimetric assay is much more sensitive than the conventional AChE assay kit, we adapted this assay for detecting enterovirus 71 (EV71) in complex samples. EV71 is the major causative agent of hand, foot, and mouth disease (HFMD). Acute EV71 infection may cause severe neurological complications, leading to a high

mortality rate (82–94%) in severe cases.[13] Therefore, the rapid identification of EV71 infection is extremely important to enable timely treatment and predict the severity of the epidemics.

Herein, varying concentrations of EV71 (10^4–10^8 copies/mL) were first added into phosphate buffered saline (PBS) and healthy human throat swab (HTS) solutions. PBS-only and HTS-only samples were set as the blanks. HTS was used, as it is the most common clinical sample used for EV71 detection. In both cases, the color of the AuNP solutions changed from red to purple, which can be easily differentiated by the naked eye (Figure 2a). In terms of the blank sample,

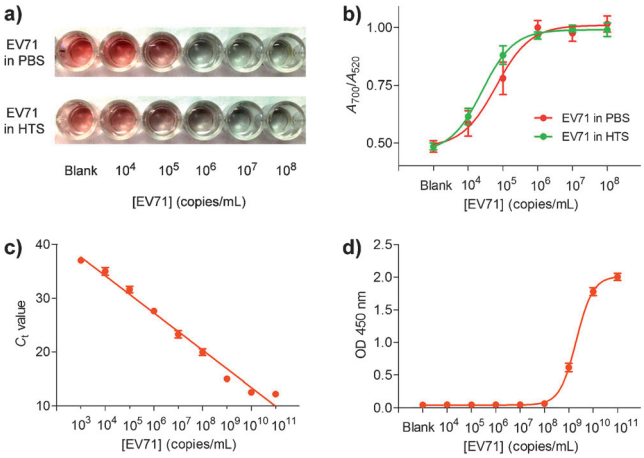

Figure 2. Detection of EV71 in spiked samples by different methods. a) Color-based detection of EV71 with concentrations of 10^4–10^8 copies/mL in phosphate buffered saline (PBS) and human throat swab (HTS) by AuNP-based sandwich ELISA assay. Samples of PBS and HTS without EV71 were used as blanks. b) A_{700}/A_{520} values versus different concentrations of EV71 in PBS. c) Real-time polymerase chain reaction detection of EV71 in HTS and d) HRP-based ELISA detection of EV71. Error bars show the standard deviations of three independent measurements.

the solution remained red because neither Ab1 nor Ab2 can specifically recognize the unknown matrices in HTS solutions, thus demonstrating that the unknown components in clinical samples have negligible effects on detection. Therefore, we can conclude that the color change of the solutions is based on the biospecific interactions between EV71 and its antibodies, rather than the nonspecific interactions between Ab2-AChE-MB and the polystyrene (PS) surfaces. The lowest concentration of EV71 where the color change can be discriminated by the naked eye was 10^4 copies/mL. Moreover, the color change of solutions was strongly associated with the change in UV/Vis absorbance (Figure 2b). By measuring the A_{700}/A_{520} value for each sample, we observed that the A_{700}/A_{520} values for both EV71-spiked PBS and HTS samples had a similar trend: increasing gradually from around 0.5 to 1.0 as the amount of EV71 added was increased. When we applied Ab2-coated MB instead of Ab2-AChE-MB in EV71 detection, no color change was observed (Figure S8). The results indicated that the color change of AuNP slutions was attributable to the presence of AChE on MB, and that the MB itself has negligible effect on the colorimetric assay.

Presently, real-time PCR (RT-PCR) is the gold standard for diagnosing HFMD, as well as many other infectious diseases in the clinic. As shown in Figure 2c, the lowest detectable concentration of EV71 using RT-PCR was 10^3 copies/mL, about one order of magnitude lower than that of the AuNP-based colorimetric assay. Although RT-PCR is an outstanding amplification platform for the detection of RNA residing in the EV71 particles, it requires expensive equipment and reagents, and complex analytical techniques, which may not be available in resource-poor settings. Horseradish peroxidase (HRP)-based ELISA, the most commonly used approach for clinical biomarker detection, was compared with our colorimetric assay. The lowest detectable concentration of EV71 using HRP-based ELISA was found to be 10^8 copies/mL (Figure 2d), which was four orders of magnitude higher than that of the AuNP-based colorimetric assay.

Encouraged by the outstanding sensitivity of this AuNP-based colorimetric assay, which is comparable to RT-PCR, we tested the capability of this assay in the clinical diagnosis of HFMD patients (Table S1) that suffered from EV71 infection. These cases had been positively diagnosed using RT-PCR. Five unrelated HTS samples collected from patients who suffered from influenza A, and five other healthy HTS samples were used as controls. HRP-based ELISA was used to screen the same clinical samples to compare with our assay. We differentiated positive and negative samples on the basis of the clinical threshold, which is indicated by the horizontal dotted line in Figure 3a. As can be seen, 28 out of 34 EV71 cases were positively detected by the AuNP-based colorimetric assay; that is, the A_{700}/A_{520} values are above the clinical threshold (where the A_{700}/A_{520} value was 0.53). Meanwhile, the A_{700}/A_{520} values for both influenza A and healthy HTS samples were below the clinical threshold, indicating that our assay offers excellent clinical specificity (100%) and sensitivity (82.3%). In comparison, the HRP-based ELISA format failed to give positive absorbance signals for any of the clinical samples (Figure 3b). The ELISA results are not surprising because of its moderate detection sensitivity, which cannot reach the clinical threshold concentrations of EV71 in clinical samples.

Coxsackievirus A16 (CA16) is another etiological agent of HFMD that is closely related to EV71, but which causes fewer infection outcomes than EV71.[14] The accurate differentiation of these two types of virus is extremely meaningful for making clinical decisions. We developed two parallel sets of assays based on the AuNP-based colorimetric strategy for CA16 (17 HTS samples) and EV71 (18 HTS samples), respectively, and evaluated their detection sensitivity and specificity. In the assay specifically designed for EV71, the sensitivity was found to be 83.3%, along with specificity of 94.1% (with a 95% confidence interval of 81.9–100.0%; Figure S9a,c). Whereas the sensitivity and specificity for CA16, where the Ab1 and Ab2 were specifically designed for CA16, were 76.5% and 83.3% (with 95% confidence interval of 69.8–97.6%), respectively (Figure S9b,d). More details are shown in Tables S2 and S3. These results revealed that our

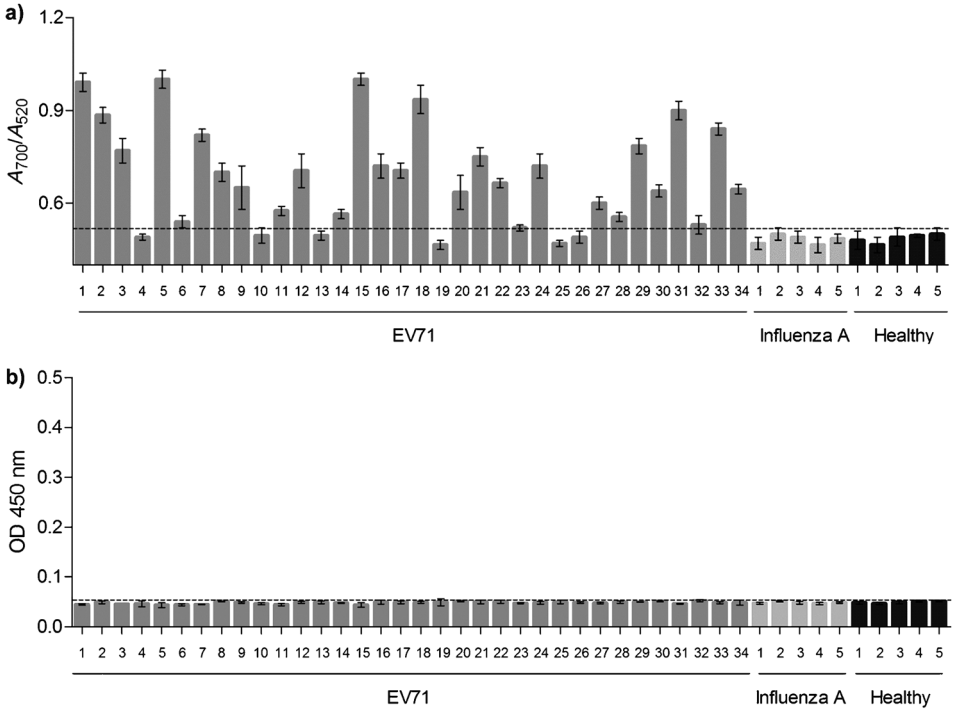

Figure 3. Clinical detection of EV71 by AuNP-based assay. HTS clinical samples collected from 34 EV71-infectious HFMD patients, 5 influenza A patients (control), and 5 healthy individuals (control) were used to evaluate the detection performance of the AuNP-based colorimetric assay (a) and the conventional HRP-based ELISA (b). Error bars show the standard deviations of three independent measurements.

colorimetric assay has the ability to specifically diagnose HFMD infected by EV71 or CA16. Given the distinct advantages of high sensitivity and specificity, convenient readout (with the naked eye and/or UV/Vis absorption), speed, and economy, this AuNP-based colorimetric assay holds great promise as an alternative to RT-PCR for clinical diagnosis of HFMD and other infectious diseases.

In conclusion, we have developed an ultrasensitive colorimetric assay for pathogen detection based on an AChE-catalyzed hydrolysis reaction. The detection sensitivity of this assay is comparable to that of RT-PCR. Moreover, this assay offers at least two advantages over RT-PCR: 1) it does not require the handling of RNA and accurate control of temperature, thus avoiding cross-contamination; 2) RT-PCR not only requires expensive instruments and reagents to acquire the results, but also needs an in-depth understanding of normalization techniques for analyzing the obtained results, whereas the colorimetric assay is based on the naked eye alone, without resorting to advanced instruments or complex analysis techniques. Considering the high detection sensitivity and convenient readout, our assay has great potential to replace RT-PCR in many cases. In addition, this assay is conducted in a 96-well plate, the most popular detection format in clinical laboratories, making this assay easily adaptable into the currently available ELISA platforms that are commonly used in resource-poor settings.

Received: September 10, 2013
Published online: October 23, 2013

Keywords: acetylcholinesterase · analytical methods · gold · hydrolysis · nanoparticles

[1] a) J. F. Rusling, *Anal. Chem.* **2013**, *85*, 5304 – 5310; b) N. L. Rosi, C. A. Mirkin, *Chem. Rev.* **2005**, *105*, 1547 – 1562; c) Y. Xiang, Y. Lu, *Nat. Chem.* **2011**, *3*, 697 – 703; d) S. Song, Z. Liang, J. Zhang, L. Wang, G. Li, C. Fan, *Angew. Chem.* **2009**, *121*, 8826 – 8830; *Angew. Chem. Int. Ed.* **2009**, *48*, 8670 – 8674.

[2] K. Hsieh, A. S. Patterson, B. S. Ferguson, K. W. Plaxco, H. T. Soh, *Angew. Chem.* **2012**, *124*, 4980 – 4984; *Angew. Chem. Int. Ed.* **2012**, *51*, 4896 – 4900.

[3] a) B. Lam, J. Das, R. D. Holmes, L. Live, A. Sage, E. H. Sargent, S. O. Kelley, *Nat. Commun.* **2013**, *4*, 2001; b) X. Guo, A. Kulkarni, A. Doepke, H. B. Halsall, S. Iyer, W. R. Heineman, *Anal. Chem.* **2012**, *84*, 241 – 246.

[4] a) L. Chen, X. Zhang, G. Zhou, X. Xiang, X. Ji, Z. Zheng, Z. He, H. Wang, *Anal. Chem.* **2012**, *84*, 3200 – 3207; b) K. Zagorovsky, W. C. W. Chan, *Angew. Chem.* **2013**, *125*, 3250 – 3253; *Angew. Chem. Int. Ed.* **2013**, *52*, 3168 – 3171; c) J. H. Jung, D. S. Cheon, F. Liu, K. B. Lee, T. S. Seo, *Angew. Chem.* **2010**, *122*, 5844 – 5847; *Angew. Chem. Int. Ed.* **2010**, *49*, 5708 – 5711; d) H. J. Chung, C. M. Castro, H. Im, H. Lee, R. Weissleder, *Nat. Nanotechnol.* **2013**, *8*, 369 – 375.

[5] E. L. Tan, L. L. Yong, S. H. Quak, W. C. Yeo, V. T. Chow, C. L. Poh, *J. Clin. Virol.* **2008**, *42*, 203 – 206.

[6] a) R. Elghanian, J. J. Storhoff, R. C. Mucic, R. L. Letsinger, C. A. Mirkin, *Science* **1997**, *277*, 1078 – 1081; b) R. de La Rica, M. M. Stevens, *Nat. Nanotechnol.* **2012**, *7*, 821 – 824; c) A. Laromaine, L. L. Koh, M. Murugesan, R. V. Ulijn, M. M. Stevens, *J. Am. Chem. Soc.* **2007**, *129*, 4156 – 4157; d) J. W. Liu, Y. Lu, *Angew. Chem.* **2006**, *118*, 96 – 100; *Angew. Chem. Int. Ed.* **2006**, *45*, 90 – 94; e) D. Li, A. Wieckowska, I. Willner, *Angew. Chem.* **2008**, *120*, 3991 – 3995; *Angew. Chem. Int. Ed.* **2008**, *47*, 3927 – 3931; f) D. Liu, W. Chen, K. Sun, K. Deng, W. Zhang, Z. Wang, X. Jiang, *Angew. Chem.* **2011**, *123*, 4189 – 4193; *Angew. Chem. Int. Ed.* **2011**, *50*, 4103 – 4107; g) Y. Jiang, H. Zhao, Y. Lin, N. Zhu, Y. Ma, L. Mao, *Angew. Chem.* **2010**, *122*, 4910 – 4914; *Angew. Chem. Int. Ed.* **2010**, *49*, 4800 – 4804.

[7] D. Liu, W. Qu, W. Chen, W. Zhang, Z. Wang, X. Jiang, *Anal. Chem.* **2010**, *82*, 9606 – 9610.

[8] a) S. Krishnan, V. Mani, D. P. Wasalathanthri, C. V. Kumar, J. F. Rusling, *Angew. Chem.* **2011**, *123*, 1207 – 1210; *Angew. Chem. Int. Ed.* **2011**, *50*, 1175 – 1178; b) V. Mani, D. P. Wasalathanthri, A. A. Joshi, C. V. Kumar, J. F. Rusling, *Anal. Chem.* **2012**, *84*, 10485 – 10491.

[9] J. M. Baskin, J. A. Prescher, S. T. Laughlin, N. J. Agard, P. V. Chang, I. A. Miller, A. Lo, J. A. Codelli, C. R. Bertozzi, *Proc. Natl. Acad. Sci. USA* **2007**, *104*, 16793 – 16797.

[10] M. Wang, X. Gu, G. Zhang, D. Zhang, D. Zhu, *Langmuir* **2009**, *25*, 2504 – 2507.

[11] G. L. Ellman, K. D. Courtney, V. Andres, R. M. Featherstone, *Biochem. Pharmacol.* **1961**, *7*, 88 – 95.
[12] X. Liu, M. Atwater, J. Wang, Q. Huo, *Colloids Surf. B* **2007**, *58*, 3 – 7.
[13] F. C. Zhu, Z. L. Liang, X. L. Li, H. M. Ge, F. Y. Meng, Q. Y. Mao, Y. T. Zhang, Y. M. Hu, Z. Y. Zhang, J. X. Li, F. Gao, Q. H. Chen, Q. Y. Zhu, K. Chu, X. Wu, X. Yao, H. J. Guo, X. Q. Chen, P. Liu, Y. Y. Dong, F. X. Li, X. L. Shen, J. Z. Wang, *Lancet* **2013**, *381*, 1037 – 1045.
[14] S. Wu, N. Duan, X. Ma, Y. Xia, Y. Yu, Z. Wang, H. Wang, *Chem. Commun.* **2012**, *48*, 4866 – 4868.

